ANTHROPOLOGY

Co-occurrence of Acheulian and Oldowan artifacts with *Homo erectus* cranial fossils from Gona, Afar, Ethiopia

Sileshi Semaw[1,2]*, Michael J. Rogers[3], Scott W. Simpson[4,5], Naomi E. Levin[6], Jay Quade[7], Nelia Dunbar[8], William C. McIntosh[8], Isabel Cáceres[9,10], Gary E. Stinchcomb[11], Ralph L. Holloway[12], Francis H. Brown[13†], Robert F. Butler[14], Dietrich Stout[15], Melanie Everett[16]

Although stone tools generally co-occur with early members of the genus *Homo*, they are rarely found in direct association with hominins. We report that both Acheulian and Oldowan artifacts and *Homo erectus* crania were found in close association at 1.26 million years (Ma) ago at Busidima North (BSN12), and ca. 1.6 to 1.5 Ma ago at Dana Aoule North (DAN5) archaeological sites at Gona, Afar, Ethiopia. The BSN12 partial cranium is robust and large, while the DAN5 cranium is smaller and more gracile, suggesting that *H. erectus* was probably a sexually dimorphic species. The evidence from Gona shows behavioral diversity and flexibility with a lengthy and concurrent use of both stone technologies by *H. erectus*, confounding a simple "single species/single technology" view of early *Homo*.

INTRODUCTION

The Gona Project study area, Afar, Ethiopia, has yielded numerous Oldowan archaeological occurrences from 2.6 to 2.0 million years (Ma) ago (*1*). Study of sediments younger than 2.0 Ma ago at Gona can contribute to understanding Mode 2 (Acheulian) technological emergence and evolution and the makers of this technology (*2*). We previously reported a pelvis from Gona, furthering our understanding of *Homo erectus* pelvic morphology and evolutionary biology (*3*). Here, we report combined Oldowan (Mode 1) and Acheulian (Mode 2) stone tool assemblages and hominin cranial fossils found in direct association that derive from stratigraphic levels dating to 1.26 Ma ago at Busidima North (BSN12) and approximately 1.6 to 1.5 Ma ago at Dana Aoule North (DAN5) (*4*, *5*) (Figs. 1 and 2 and figs. S1 and S2), which illuminate *H. erectus* variability and behavioral flexibility.

RESULTS

DAN5 and BSN12 sites at Gona: Stratigraphy and archaeology

Abundant stone artifacts, fossil fauna, and a hominin partial calvarium (BSN12/P1) were found at BSN12 (Figs. 3 and 4) in direct association with the Boolihinan Tuff (BHT) (*4*). Mode 1 artifacts were recovered in situ from the BHT, and glass shards of tephra that geochemically match the BHT were found cemented onto the BSN12/P1 parietal and on both Mode 1 and Mode 2 artifacts (Figs. 3 and 4, fig. S1, sections S1 to S4, and auxiliary data file 1A). Twenty-eight meters of reversely magnetized sediments overlie the BHT, capped by an additional 18+ m of normally magnetized sediments that we assign to the upper Matuyama and Brunhes Chrons, respectively (Fig. 2 and auxiliary data file 1B). Normally magnetized sediments occur 6 m below the BHT, which we interpret to represent the Olduvai Subchron (1.95 to 1.78 Ma ago) (*4*). The BHT shows strong geochemical affinities with a tuff from Melka Kunture, Ethiopia, dated to 1.262 ± 0.034 Ma ago (1σ uncertainty on ages reported here and elsewhere in text) (*5*) (auxiliary data file 1, A and B, and sections S1 to S3), consistent with its stratigraphic position in the middle of the Matuyama Chron.

At the DAN5 locality, ~5.7 km northeast of BSN12 (figs. S2 to S5), a well-preserved hominin cranium DAN5/P1 (Fig. 3) and both Mode 1

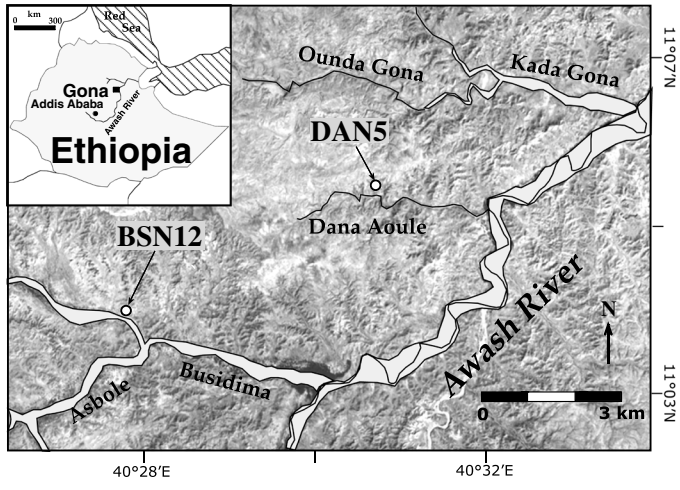

Fig. 1. Map of the Gona study area, showing the locations of the DAN5 and BSN12 hominin and archaeological localities.

[1]Centro Nacional de Investigación sobre la Evolución Humana (CENIEH), Sierra de Atapuerca 3, 09002 Burgos, Spain. [2]Stone Age Institute and CRAFT Research Center, 1392 W. Dittemore Rd., Gosport, IN 47408, USA. [3]Department of Anthropology, Southern Connecticut State University, 501 Crescent Street, New Haven, CT 06515, USA. [4]Department of Anatomy, Case Western Reserve University School of Medicine, Cleveland, OH 44106, USA. [5]Laboratory of Physical Anthropology, Cleveland Museum of Natural History, Cleveland, OH 44106, USA. [6]Department of Earth and Environmental Sciences, University of Michigan, 1100 North University Avenue, Ann Arbor, MI 48109, USA. [7]Department of Geosciences/Desert Laboratory, University of Arizona, Tucson, AZ 85721, USA. [8]New Mexico Bureau of Geology and Mineral Resources, Earth and Environmental Science Department, New Mexico Tech, 801 Leroy Place, Socorro, NM 87801-4796, USA. [9]Universitat Rovira i Virgili (URV), Avinguda de Catalunya 35, 43002 Tarragona, Spain. [10]IPHES, Institut Català de Paleoecologia Humana i Evolució Social, Zona Educacional 4–Campus Sescelades URV (Edifici W3), 43007 Tarragona, Spain. [11]Watershed Studies Institute and Department of Earth and Environmental Sciences, Murray State University, Murray, KY 42071, USA. [12]Department of Anthropology, Columbia University, 1200 Amsterdam Ave., New York, NY 10027, USA. [13]The University of Utah, 201 South Presidents Circle Room 201, Salt Lake City, UT 84112, USA. [14]Department of Physics, University of Portland, Portland, OR 97203, USA. [15]Department of Anthropology, Emory University, 1557 Dickey Drive, Atlanta, GA 30322, USA. [16]Chevron Energy Technology Company, 1500 Louisiana St., Houston, TX 77002, USA.
*Corresponding author. Email: sileshi.semaw@cenieh.es
†Deceased.

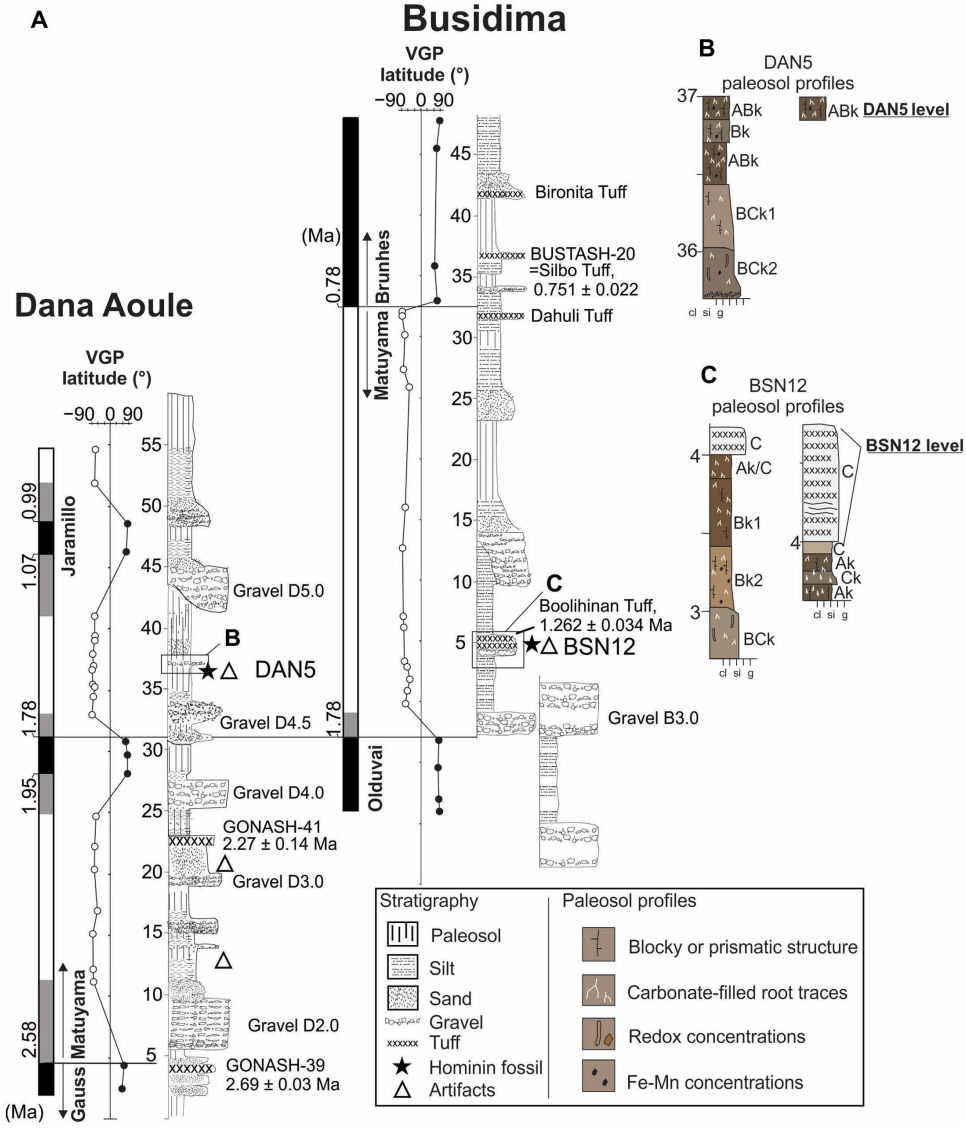

Fig. 2. Relevant stratigraphy for the BSN12 and DAN5 archaeological sites at Gona. (**A**) Composite stratigraphic sections through Dana Aoule and the BSN12 areas. Positions of fossil crania (DAN5 and BSN12) are shown, as well as volcanic tuffs and their ages in millions of years, and errors (1σ), from (*4*) and (*5*). Virtual geomagnetic pole (VGP) latitude is indicated for paleomagnetic samples, and their proposed correlations to the geomagnetic time scale are indicated for each section. (**B**) and (**C**) provide detailed stratigraphies of the DAN5 and BSN12 hominin and archaeological localities.

and Mode 2 artifacts associated with cutmarked bones (sections S4 and S5) were found eroding in weakly developed paleosols that were later buried and overprinted by a well-developed vertic paleosol (Fig. 2, fig. S4, sections S6 and S7, and auxiliary data file 1, C to E, for paleosol descriptions of both the DAN5 and BSN12 sites). Although much of the cranium was found on the surface, the occipital and left maxilla were found in situ, along with six manuports and one Oldowan core (figs. S2 to S5). Freshly eroded Mode 1 and Mode 2 artifacts and fauna were also collected at the DAN5 hominin site, DAN5-South (~140 m south-southwest), and DAN5-West (~50 m west-northwest), all within the same general stratigraphic context, and subsequent site visits yielded additional freshly eroded artifacts and fauna bearing evidence of stone tool cutmarks. All the DAN5 area artifacts and fossils were found in close proximity and from the same stratigraphic interval within a fining upward sequence (Fig. 2 and figs. S2 to S5). The DAN5 artifacts and fossils come from a siltstone unit in reversed magnetized sediments 6.5 m above the top of the Olduvai Subchron and 10.5 m below the base of the Jaramillo Subchron (*4*), with a well-developed, 8- to 9-m-thick, cumulic paleosol separating the artifacts and cranium from the normally magnetized stratigraphic interval above (Fig. 2). The DAN5 artifacts and cranium are constrained between 1.78 and 1.07 Ma. Using average local sedimentation rates (auxiliary data file 1B), the age estimate of DAN5 can be interpolated and narrowed to ~1.6 to 1.5 Ma (*4*). This estimate is reasonable, given the thick paleosol and gravel that separate DAN5 from the base of the Jaramillo Subchron above and the stratigraphic proximity to the underlying Olduvai Subchron (Fig. 2 and sections S1 to S3).

The DAN5 and BSN12 stone tool assemblages include Mode 2 handaxes and picks ("large cutting tools" or LCTs) and Mode 1 artifacts (unshaped cores and débitage) (Fig. 4, Table 1, and section S4).

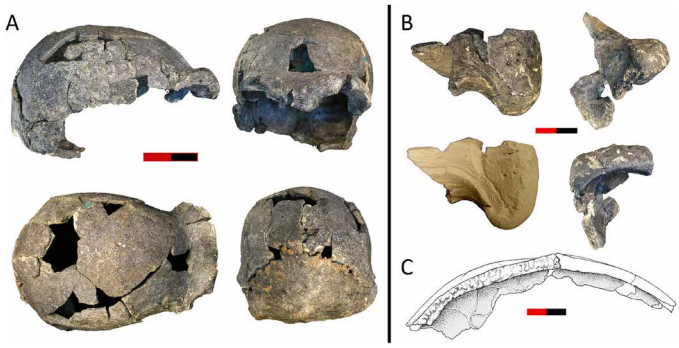

Fig. 3. Hominin crania. (**A**) DAN5/P1 neurocranium—four views: lateral, frontal, superior, and posterior. (**B**) BSN12/P1 frontal—three views: superior (original fossil and cast), lateral, and frontal. (**C**) BSN12/P1 vault—conjoined parietal and frontal viewed along midline anterior—is to the right. Scale bars, 40 mm (DAN5/P1) and 20 mm (BSN12/P1). For additional views, see the Supplementary Materials. Photo Credit: Scott W. Simpson, Case Western Reserve University.

The two Gona sites highlighted here were close to riverine sources of raw materials containing trachyte, rhyolite, and basalt cobbles from which most of the artifacts were made. The DAN5 LCTs share broad similarities with those from other early Acheulian sites, such as Konso (Ethiopia) (*6*) and Kokiselei (Kenya) (*7*), but differ in some details (table S1). About half of the DAN5 and BSN12 handaxes were made on cobbles, whereas a majority of the handaxes at the 1.75-Ma and younger Konso sites were flake-based (*6*). A majority of the DAN5 handaxes (87%) were bifacially worked, with better representation of unifacial flaking at Konso. The early Konso handaxes also appear to be longer on average and slightly thinner than those of DAN5. The differences between the Gona and Konso assemblages probably relate to raw material characteristics (flakes from large boulders used at Konso versus smaller cobbles used more often at Gona).

DAN5 and BSN12 hominin crania

The larger BSN12/P1 (Fig. 3, fig. S6, sections S8 and S9, and table S2) adult calvarium includes portions of the right orbital margin, frontal squama, and left parietal. The BSN12/P1's robust supraorbital torus is less arched and thickens laterally where it is joined by the temporalis lines. There is slight sagittal keeling of the vault with some thickening at bregma and parasagittal flattening of the parietal. Endocranial volume is estimated to be between 800 and 900 ml. The robusticity of the supraorbital torus suggests that the individual was a male.

The more complete DAN5/P1 cranium includes much of the vault and maxillae with right P4-M1 and left P3-M3 (Fig. 3, fig. S7, sections S8 and S9, and tables S2 and S3). The vault is globular with an arching supraorbital torus that thins laterally and projects anteriorly forming a well-defined post-toral sulcus. The small endocranial volume (~598 ml) makes it the smallest adult erectin known from Africa (fig. S7). The vault lacks evidence of sagittal keeling although there is a midline parietal swelling above lambda. The vault is thickened at asterion, and lambda and angular tori are present. The anterior margin of the zygomatic root is transversely oriented, and the absence of anterior inflation of the maxillary sinus produces a deep canine fossa. Although the canine is missing, its alveolus is short and ends below the nasal floor indicating a small root. The combination of a gracile neurocranium and face along with a small canine alveolus suggests that this individual was female.

The smaller more gracile DAN5/P1 and the larger more robust BSN12/P1 crania share derived anatomical features diagnostic for *H. erectus*, yet they differ in several ways (e.g., overall size, details of supraorbital torus robusticity and morphology, sagittal and coronal contours of the vault, degree of midline keeling, and course of the temporalis lines) that require further comment (see sections S8 and S9). The DAN5/P1 cranium bears similarity to the 1.85- to 1.76-Ma Dmanisi crania (*8*, *9*), the 1.6- to 1.5-Ma juvenile KNM-ER 42700 (*10*), and the small 0.95-Ma Olorgesailie [KNM-OL 45500 (*11*)] *H. erectus* crania, and it differs from the typical Asian *H. erectus* crania by having a smaller endocranial volume, a weakly flexed occipital, and lack of continuous mound-like occipital torus—characters that may correlate with overall size (*10*, *12*). The BSN12/P1 fossil is similar to the more robust African specimens such as Olduvai Hominid 9, the ca. 1-Ma specimens from Middle Awash, Ethiopia [BOU-VP-2/66 (*13*)] and Buia, Eritrea [UA-31 (*14*)], and those from Indonesia and eastern Asia by having a longer and lower vault with a thickened supraorbital torus. This anatomical variation in the Gona specimens can be interpreted in several ways. First, the older DAN5/P1 individual may retain more primitive anatomy (e.g., smaller size, gracile vault, and thin supraorbital tori) than the younger BSN12/P1 fossil, and this variation is due to secular anagenetic evolutionary trends within African *H. erectus*. Alternatively, the size and anatomical variation observed in the Gona specimens is primarily a consequence of sexual dimorphism within a single species. Last, these fossils might reflect a degree of taxonomic diversity previously unrecognized in the Afar for the genus *Homo* (*15*).

Paleoenvironmental settings

At DAN5, the combination of stratigraphic proximity to a thick cobble conglomerate, the associated fauna (table S4), and data from paleosols is consistent with an ancient landscape that included riparian woodlands with edaphic grasslands (sections S6 and S7 and auxiliary data file 1, C to E). The fauna recovered from the BSN12 site (table S4) shows a strong preference for more open dry and wet grassland habitats, consistent with the bulk geochemistry and $\delta^{13}C$ values from associated soil carbonates (*16*) and fossil teeth (auxiliary data file 1, F to H). In summary, the paleoenvironmental information indicates that hominin toolmakers lived in close proximity to ancient rivers, with riparian woodlands adjacent to open habitats.

The stable isotope values of the DAN5/P1 maxillary right first molar ($\delta^{13}C = -9.2‰$ and $\delta^{18}O = -2.0‰$) are consistent with a diet dominated by C_3 plants or, alternatively, broad spectrum omnivory (e.g., eggs, insects, and browsing herbivores). The $\delta^{13}C$ value from DAN5/P1 is among the lowest $\delta^{13}C$ values for early Pleistocene *Homo* teeth that have been sampled (*17*, *18*). It is within the range of $\delta^{13}C$ values from *Homo* for specimens older than 1.65 Ma ago (−9.9 to −3.9‰, identified to *Homo* sp. indet. from the Turkana Basin and *Homo rudolfensis* from the Malawi Rift), but it is lower than the $\delta^{13}C$ values for *Homo* < 1.65 Ma ago, which have only been reported from the Turkana Basin (−4.3 ± 1.1‰; range, −5.6 to −2.6‰; $n = 10$). While the low $\delta^{13}C$ value from DAN5/P1 is noteworthy given higher $\delta^{13}C$ values from contemporaneous *Homo* in Turkana (indicating consumption of more C_4 resources there), in our view, there is not enough isotopic data for *Homo* from this time period to make further interpretations from this single Gona sample. However, if this low $\delta^{13}C$ value from DAN5/P1 were more broadly represented in subsequent sampling, then it would be indicative of a broad, varied diet. Additional isotopic data from more specimens and from a greater geographic range are needed to put the data from DAN5/P1 into context.

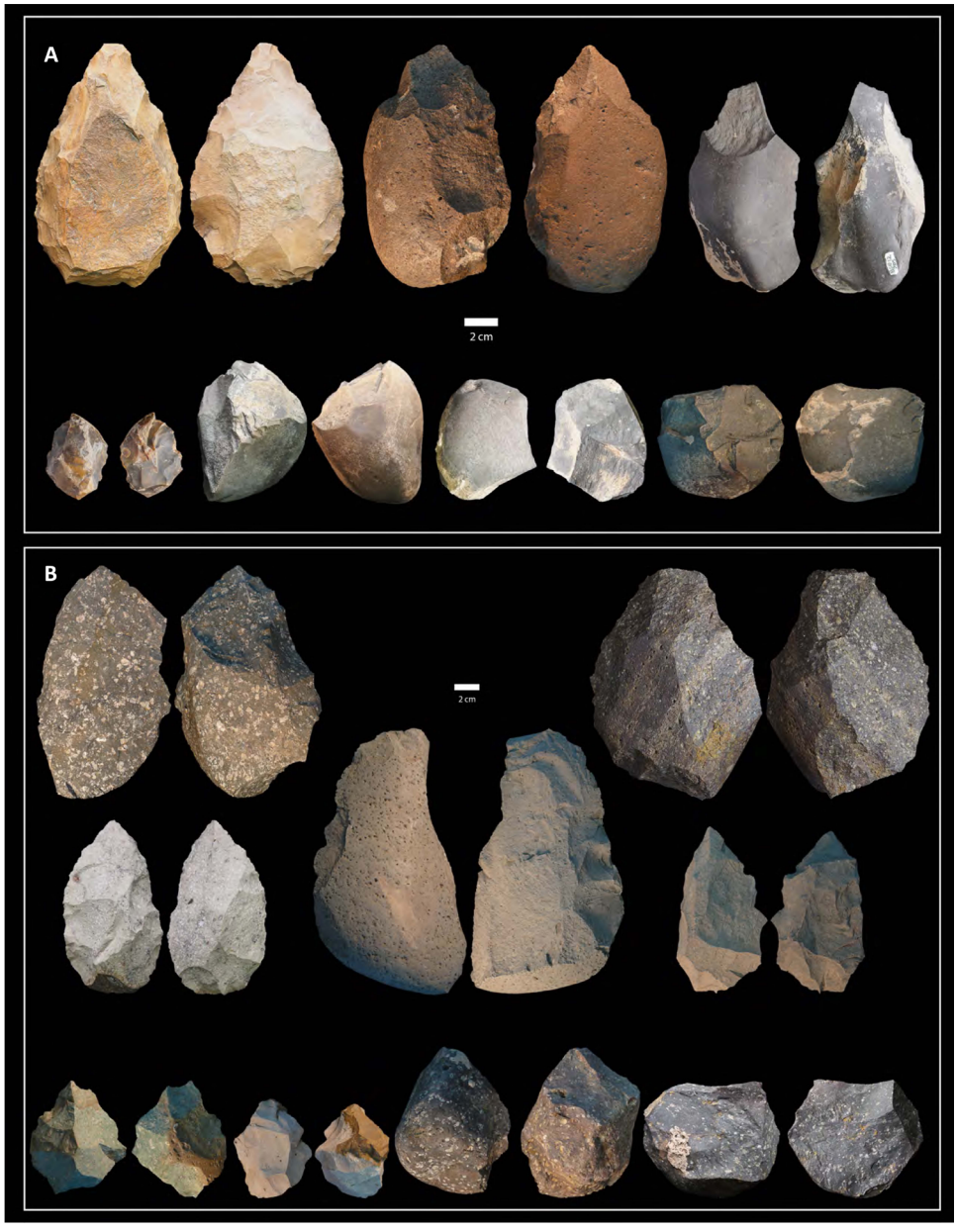

Fig. 4. Diagnostic stone artifacts. Two opposing views of Acheulian (Mode 2) and Oldowan (Mode 1) stone tools from (**A**) BSN12 and (**B**) DAN5. For each site, the Mode 1 cores are on the bottom row. Photo Credit: Michael J. Rogers, Southern Connecticut State University.

DISCUSSION

At this time, we interpret the marked anatomical variability between DAN5/P1 and BSN12/P1 to be a consequence of a widely dispersed, long-lived, sexually dimorphic species. The earlier Dmanisi sample also shows a remarkable degree of size and sexual dimorphism within a sample of *H. erectus* (*8*, *9*). The broad dispersion and probable low population density of *H. erectus* created opportunities for developing regional anatomical morphs due to periods of interrupted gene flow. As shown by recent studies of ancient DNA, hominins can and will recognize each other as viable mates even after many hundreds of thousands of years of separation (*19*), such that a temporary interruption in gene flow does not necessarily result in speciation. This interrupted mixing of genes between small, dispersed groups can lead to a highly polymorphic species that will share many major anatomical and behavioral attributes but still express a great degree of phenetic variation.

The archaeological record at Gona is broadly consistent with this scenario, as the co-occurrence of Mode 1 and Mode 2 stone tools with *H. erectus* over time suggests variably conserved behavioral traits and traditions among small, dispersed populations. Early Acheulian sites almost always have Mode 1 cores and flakes found in association with LCTs, with varying abundances documented at sites such as Konso (*6*), Kokiselei (*7*), and Melka Kunture (Garba IV D site) (*20*). In addition, it is our observation at Gona and elsewhere that many archaeological sites dating to 1.6 to 0.5 Ma ago only contain Mode 1 stone tools, although these sites are probably underreported. The

Table 1. Composition of the BSN12 and DAN5 artifact assemblages. Surface artifacts are likely from the same stratigraphic context as the hominin fossils, although confidence in this assessment is low. "In context" artifacts are confidently considered to be from the same stratigraphic context as the hominin fossil site because they (i) were excavated in situ [5 artifacts from BSN12A and 11 from DAN5 (Main [M] and West [W])], (ii) were found encased in the BHT (at BSN12), or (iii) were recovered after refreshing from previously surface-scraped areas after subsequent biennial site revisits, such as at DAN5-South (S), DAN5-M, and DAN5-W.

Artifact type	**BSN12 in context**	BSN12 surface	***BSN12 total***	**DAN5-M in context**	DAN5-M surface	**DAN5 (S & W) in context**	DAN5 (S & W) surface	***DAN5 total***
Handaxes	**1**	2	*3*	**3**	3	**6**	3	*15*
Picks	**1**	0	*1*	**3**	0	**1**	1	*5*
Cleavers	**0**	0	*0*	**0**	0	**0**	2	*2*
Retouched large flakes/ knives	**0**	0	*0*	**0**	0	**1**	2	*3*
Mode 1 cores	**12**	25	*37*	**3**	5	**3**	9	*20*
Whole flakes	**10**	90	*100*	**0**	3	**3**	15	*21*
Retouched flakes/ scrapers	**1**	5	*6*	**0**	0	**0**	1	*1*
Flake fragments	**10**	39	*49*	**0**	4	**3**	13	*20*
Core fragments	**1**	2	*3*	**0**	1	**0**	1	*2*
Cobbles	**0**	0	*0*	**6**	0	**3**	6	*15*
Broken/split cobbles	**3**	0	*3*	**0**	0	**0**	0	*0*
Totals	**39**	163	*202*	**15**	16	**20**	53	*104*

Gona evidence suggests that most of these Mode 1 sites were created by *H. erectus* (sensu lato), not a different hominin species, particularly in areas that do not preserve evidence of other hominins in the Middle Pleistocene, such as the Afar.

Seeing the expression of *H. erectus* stone tool technology as variable, flexible [e.g., (*21*)], and a reflection of many different factors (such as site sampling sizes, tool function, distance to stone raw material sources, environmental variability, population size, degree of contact with other groups, etc.) can help demystify this observed pattern, as well as observations of seemingly "advanced" LCTs (i.e., symmetrical, thin, and/or invasively flaked) found alongside "crude" LCTs (e.g., at FLK-West, BSN12, and DAN5) and the lack of LCTs at some sites outside of Africa.

Some early hominin populations, including small groups of *H. erectus*, left Africa, making it to Eurasia by ~1.8 Ma ago [e.g., at Dmanisi (*22*)]. Given the early age of the Dmanisi site, it is possible that the population that left for Eurasia departed Africa by ~1.8 to 1.9 Ma ago, i.e., before the development of the Acheulian. Thus, the group(s) that remained in Africa most likely developed Acheulian technology, which was later carried along via subsequent waves of migrations to Asia [e.g., (*23*)]. Some researchers (*7*) also hypothesized that multiple hominin species may have been responsible for two distinct contemporary technologies. To the contrary, we argue here that the same hominin species, *H. erectus*, that remained in Africa invented the Acheulian, variably and flexibly using both Mode 1 and Mode 2 stone technologies, a view also shared by others [e.g., (*6*)].

At a basic level, Acheulian toolmakers created handaxes and picks using large-sized raw materials, with complex execution demanding advanced hierarchical organization (*24*), while also creating Mode 1 stone tools, whenever sharp-edged cutting flakes were needed. Stone tool function could be a particularly important factor in the variable expression of stone technologies. Cutmarks or hammerstone-percussed bones were not identified on the abundant BSN12 fossils. The DAN5 fauna, however, yielded two bones with modifications, showing disarticulation and defleshing from a large range of animal sizes (fig. S8, section S5, and table S5), consistent with the evidence of hominin animal consumption at FLK-West at Olduvai Bed II (Tanzania) (*25*). The evidence from Gona suggests that *H. erectus* had population-level behavioral diversity and flexibility, with a lengthy and concurrent use of both Mode 1 and Mode 2 technologies, the variable expression of which deserves continued research. Thus, further field investigations will be important to find additional fossil hominins and their cultural remains in the 2.0- to 1.0-Ma time interval.

MATERIALS AND METHODS

Methods

Microprobe analysis

Tuffs were first treated with 2 M HCl to remove any carbonate, briefly rinsed in 2% HF, and washed in distilled water. Glass were separated into size fractions of >120, 60 to 120, and <60 μm. All glass analyses were carried out using a Cameca SX-100 electron microprobe located at New Mexico Institute of Mining and Technology following sample preparation as described in (*26*). Samples were examined using backscattered electron imagery, and selected particles were quantitatively analyzed. Elements analyzed include Na, Mg, Al, Si, P, S, Cl, K, Ca, Ti, Mn, and Fe. An accelerating voltage of 15 kV and a probe current of 10 nA were used. Beam sizes of between 10 and 20 μm were used to avoid Na volatilization (*27*). Analytical details have been listed in footnotes of auxiliary data file 1A. We noted that analyses of many

of these tephra have been reported in previous publications but all analyses of all relevant tephra were repeated using the above procedures. Trace element analysis on a single bulk sample of volcanic ash, treated as described above, was carried out using the x-ray fluorescence method at the Washington State University Peter Hooper GeoAnalytical Lab, described in detail at that laboratory's website. Powdered rock samples were fluxed with lithium tetraborate, fused into a glass bead, and then analyzed using a Thermo ARL Advant'XP+ automated sequential wavelength spectrometer. Intensities of all elements were corrected automatically for line interference and absorption effects using the fundamental parameter method. Precision of the method is typically better than 5% (relative standard deviation) for all trace elements. Because only a single sample was analyzed for trace elements, these data are included as a footnote to auxiliary data file 1A.

Paleomagnetism

Claystone and siltstone layers were sampled for paleomagnetic analyses. Four oriented samples were collected from each sedimentary horizon. In summary, 87 horizons were sampled in Dana Aoule, Busidima, and Asbole areas (auxiliary data file 1B). These data were initially reported in (*4*) and (*3*) although we report the compiled datasets and sampling locations here (Fig. 2 and auxiliary data file 1B). All samples were thermally demagnetized in ≥12 temperature steps ranging up to 580°C, and characteristic remnant magnetization (ChRM) directions for each sample were determined by principal components analysis (*28*). Site-mean ChRM directions were calculated using Fisher's statistics (*29*). Ages for geomagnetic chrons and subchrons were based on those reported in (*30*).

Stable isotope analyses

Fossil teeth were sampled at the National Museum of Ethiopia in Addis Ababa using a rotary drill with a diamond burr bit. The surface was gently abraded before sample, and the resultant powder was treated with a dilute H_2O_2 and then a weak acetic acid, with rinses between treatments, and then dried before analysis. Isotopic analyses of teeth were performed using a Kiel Device and a Thermo Delta Plus gas-source mass spectrometer at the University of Arizona, a common acid bath device and Finnigan MAT 252 mass spectrometer at the University of Utah, and a common acid bath device and a Thermo MAT 253 mass spectrometer at Johns Hopkins University. See auxiliary data file 1H (tooth enamel) for details of the methods used for particular samples. Soil carbonate nodules were collected from distinct pedogenic carbonate (Bk) horizons in paleosols at least 40 cm below the contact with the overlying unit. All soil carbonate isotope data have been published elsewhere; see auxiliary data file 1G for a list of references and a summary of results. Results are presented in standard δ notation as the per mil (‰) deviation of the sample CO_2 from the Vienna Pee Dee Belemnite standard, where $R = {}^{13}C/{}^{12}C$ or ${}^{18}O/{}^{16}O$ and $\delta = (R_{sample}/R_{standard} - 1) \times 1000$. All measurements were made relative to working carbonate and enamel reference material, and typical precision of replicate analyses was 0.1‰ for both $\delta^{13}C$ and $\delta^{18}O$ measurements.

Paleosols

Trenches in the paleosols were excavated at the DAN5 and BSN12 sites, and soil stratigraphic units were designated to identify unique paleosols, often based on evidence of paleosol burial or reversals in particle size (*31*). Paleosols associated with the DAN5 and BSN12 sites were described in the field using Natural Resources Conservation Service techniques (*32*). Samples from the DAN5 and BSN12 paleosols were selected for soil morphological and geochemical analyses to characterize the physical and chemical processes, provide inference into type of surface vegetation, and estimate paleoclimate.

Paleosol clods were selected from bulk samples and measured for bulk density using the wax clod method (*33*). The results are reported in grams per cubic centimeter and used to estimate relative changes in strain. Aliquots of bulk paleosol samples were submitted to ALS Chemex for geochemical characterization of major, trace, and rare earth elements using lithium borate fusion and inductively coupled plasma atomic emission spectroscopy and inductively coupled plasma mass spectrometry.

The DAN5 and BSN12 bulk density and geochemical data were used to determine the extent and magnitude of weathering. Mobile element additions and losses were calculated using the mass transfer coefficient, τ (*34*, *35*)

$$\tau = \frac{C_{j,w}}{C_{j,p}}\frac{C_{i,p}}{C_{i,w}} - 1 \quad (1)$$

where C is the mobile, j, or immobile, i, element concentration in the weathered, w, or parent, p, material. When $\tau = 0$, element j has not been added or removed from the profile with respect to i. When $\tau = -1$, 100% of the element j has been removed compared to i. In this study, Zr was assumed to be immobile. The ε_i for each depth interval, z, is the relative change in volume, V, between the parent and weathered portion of the profile

$$\varepsilon_i(z) = \frac{V_w - V_p}{V_p} = \frac{\rho_p}{\rho_w} * \frac{C_{i,p}}{C_{i,w}} \quad (2)$$

The ε_i was estimated using bulk density and immobile element data, $C_{i,p}$ and $C_{i,w}$, in the right-hand side of Eq. 2. The ε_i incorporated into Eq. 1 normalizes the volumetric changes that can occur during weathering, for example, dilation and collapse. The strain correction can be substantial (*36*). We estimated the paleo-pH and mean annual precipitation using bulk geochemistry from uppermost B horizons (*37*, *38*).

SUPPLEMENTARY MATERIALS

Supplementary material for this article is available at http://advances.sciencemag.org/cgi/content/full/6/10/eaaw4694/DC1

Supplementary Text
Section S1. Geologic context of sites
Section S2. Geochemistry of the BHT and stratigraphic implications
Section S3. Age determination of sites
Section S4. Additional details of the archaeological samples
Section S5. DAN5 hominin–modified bones
Section S6. Paleosols
Section S7. Ecological reconstructions
Section S8. Additional anatomical descriptions of the hominin fossils
Section S9. DAN5/P1 endocast
Section S10. Taxonomic allocation of the BSN12/P1 and DAN5/P1 specimens
Fig. S1. Setting of the BSN12 site.
Fig. S2. Map of the DAN5 area.
Fig. S3. Photographs of the original DAN5-Main discovery site.
Fig. S4. DAN5-Main area after surface brush and excavation in 2000.
Fig. S5. DAN5-Main area in 2008.
Fig. S6. BSN12/P1 partial cranium.
Fig. S7. DAN5/P1 partial cranium.
Fig. S8. Modified fossil bones from the DAN5 site complex.
Table S1. Comparison of the BSN12 and DAN5 artifacts with Konso.
Table S2. Metrical description of DAN5/P1 and BSN12/P1 specimens.
Table S3. Summary maxillary dental metrics (means and ranges) for taxa discussed in the main text.
Table S4. Fauna list from the BSN12 and DAN5 levels of the Busidima Formation, Gona.
Table S5. Taphonomic sample of fauna recovered from DAN5.
Auxiliary data file 1. Geology master data.
References (*39*–*56*)

REFERENCES AND NOTES

1. S. Semaw, P. Renne, J. W. K. Harris, C. S. Feibel, R. Bernor, N. Fesseha, K. Mowbray, 2.5-million-year-old stone tools from Gona, Ethiopia. *Nature* **385**, 333–336 (1997).
2. S. Semaw, M. J. Rogers, I. Cáceres, D. Stout, A. C. Leiss, The Early Acheulean ~1.6–1.2 Ma from Gona, Ethiopia: Issues related to the emergence of the acheulean in Africa, in *The Emergence of the Acheulean in East Africa and Beyond: Contributions in Honor of Jean Chavaillon*, R. Gallotti, M. Mussi, Eds. (Vertebrate Paleobiology and Paleoanthropology, Springer, 2018), pp. 115–128.
3. S. W. Simpson, J. Quade, N. Levin, R. Butler, G. Dupont-Nivet, M. Everett, S. Semaw, A female *Homo erectus* pelvis from Gona, Ethiopia. *Science* **322**, 1089–1092 (2008).
4. J. Quade, N. Levin, S. W. Simpson, R. Butler, W. C. McIntosh, S. Semaw, L. Kleinsasser, G. Dupont-Nivet, P. Renne, N. Dunbar, The geology of Gona, Afar, Ethiopia, in *The Geology of Early Humans in the Horn of Africa, Geological Society of America Special Paper*, J. Quade, J. G. Wynn, Eds. (The Geology Society of America, 2008), vol. 446, pp. 1–31.
5. L. E. Morgan, P. R. Renne, G. Kieffer, M. Piperno, R. Gallotti, J. P. Raynal, A chronological framework for a long and persistent archaeological record: Melka Kunture, Ethiopia. *J. Hum. Evol.* **62**, 104–115 (2012).
6. Y. Beyene, S. Katoh, G. WoldeGabriel, W. K. Hart, K. Uto, M. Sudo, M. Kondo, M. Hyodo, P. R. Renne, G. Suwa, B. Asfaw, The characteristics and chronology of the earliest Acheulean at Konso, Ethiopia. *Proc. Natl. Acad. Sci. U.S.A.* **110**, 1584–1591 (2013).
7. C. Lepre, H. Roche, D. V. Kent, S. Harmand, R. L. Quinn, J.-P. Brugal, P.-J. Texier, A. Lenoble, C. S. Feibel, An earlier origin for the Acheulian. *Nature* **477**, 82–85 (2011).
8. G. P. Rightmire, A. Margvelashvili, D. Lordkipanidze, Variation among the Dmanisi hominins: Multiple taxa or once species? *Amer. J. Phys. Anthropol.* **168**, 481–495 (2018).
9. D. Lordkipanidze, M. S. P. de León, A. Margvelashvili, Y. Rak, G. P. Rightmire, A. Vekua, C. P. E. Zollikofer, A complete skull from Dmanisi, Georgia, and the evolutionary biology of early *Homo*. *Science* **342**, 326–331 (2013).
10. F. Spoor, M. G. Leakey, P. N. Gathogo, F. H. Brown, S. C. Antón, I. McDougall, C. Kiarie, F. K. Manthi, L. N. Leakey, Implications of new early *Homo* fossils from Ileret, east of Lake Turkana, Kenya. *Nature* **448**, 688–691 (2007).
11. R. Potts, A. K. Behrensmeyer, A. Deino, P. Ditchfield, R. J. Clarke, Small mid-Pleistocene hominin associated with East African Acheulean technology. *Science* **305**, 75–78 (2004).
12. G. P. Rightmire, *Homo erectus* and Middle Pleistocene hominins: Brain size, skull form, and species recognition. *J. Hum. Evol.* **65**, 223–252 (2013).
13. B. Asfaw, W. H. Gilbert, Y. Beyene, W. K. Hart, P. R. Renne, G. WoldeGabriel, E. S. Vrba, T. D. White, Remains of *Homo erectus* from Bouri, Middle Awash, Ethiopia. *Nature* **416**, 317–320 (2002).
14. R. Macchiarelli, L. Bondioli, M. Chech, A. Coppa, A. Fiore, R. Russom, F. Vecchi, Y. Libsekal, L. Rook, The late Early Pleistocene human remains from Buia, Danakil Depression, Eritrea. *Riv. Ital. Paleontol. S.* **110**, 133–144 (2004).
15. S. C. Antón, R. Potts, L. C. Aiello, Evolution of early *Homo*: An integrated biological perspective. *Science* **345**, 1236828 (2014).
16. N. E. Levin, J. Quade, S. W. Simpson, S. Semaw, M. Rogers, Isotopic evidence for Plio–Pleistocene environmental change at Gona, Ethiopia. *Earth Planet. Sci. Lett.* **219**, 93–110 (2004).
17. T. E. Cerling, F. K. Manthi, E. N. Mbua, L. N. Leakey, M. G. Leakey, R. E. Leakey, F. H. Brown, F. E. Grine, J. A. Hart, P. Kaleme, H. Roche, K. T. Uno, B. A. Wood, Stable isotope-based diet reconstructions of Turkana Basin hominins. *Proc. Natl. Acad. Sci. U.S.A.* **110**, 10501–10506 (2013).
18. T. Lüdecke, O. Kullmer, U. Wacker, O. Sandrock, J. Feibig, F. Schrenk, A. Mulch, Dietary versatility of Early Pleistocene hominins. *Proc. Natl. Acad. Sci. U.S.A.* **115**, 13330–13335 (2018).
19. K. Prüfer, F. Racimo, N. Patterson, F. Jay, S. Sankararaman, S. Sawyer, A. Heinze, G. Renaud, P. H. Sudman, C. de Filippo, H. Li, S. Mallick, M. Dannemann, Q. Fu, M. Kircher, M. Kuhlwilm, M. Meyer, M. Ongyerth, M. Siebauer, C. Theunert, A. Tandon, P. Moorjani, J. Pickrell, J. Mullikin, S. H. Vohr, R. E. Green, I. Hellmann, P. L. F. Johnson, H. Blanche, H. Cann, J. O. Kitzman, J. Shendure, E. E. Eichler, E. S. Lein, T. E. Bakken, L. V. Golovanova, V. B. Doronichev, M. V. Shunkov, A. P. Derevianko, B. Viola, M. Slartkin, D. Reich, J. Kelso, S. Pääbo, The complete genome sequence of a Neanderthal from the Altai Mountains. *Nature* **505**, 43–49 (2014).
20. R. Gallotti, M. Mussi, Two Acheuleans, two humankinds: From 1.5 to 0.85 Ma at Melka Kunture (Upper Awash, Ethiopian highlands). *J. Archaeol. Sci.* **95**, 1–46 (2017).
21. S. C. Anton, C. W. Kuzawa, Early *Homo*, plasticity and the extended evolutionary synthesis. *Interface Focus* **7**, 20170004 (2017).
22. A. Mgeladze, D. Lordkipanidze, M.-H. Moncel, J. Despriee, R. Chagelishvili, M. Nioradze, G. Nioradze, Hominin occupations at the Dmanisi site, Georgia, Southern Caucasus: Raw materials and technical behaviours of Europe's first hominins. *J. Hum. Evol.* **60**, 571–596 (2011).
23. S. Pappu, Y. Gunnell, K. Akhilesh, R. Braucher, M. Taieb, F. Demory, N. Thouveny, Early Pleistocene presence of Acheulian Hominins in south India. *Science* **331**, 1596–1599 (2011).
24. D. Stout, N. Toth, K. D. Schick, T. Chaminade, Neural correlates of Early Stone Age tool-making: Technology, language and cognition in human evolution. *Philos. Trans. R. Soc. London Ser. B* **363**, 1939–1949 (2008).
25. F. Diez-Martín, P. S. Yusto, D. Uribelarrea, E. Baquedano, D. F. Mark, A. Mabulla, C. Fraile, J. Duque, I. Díaz, A. Pérez-González, J. Yravedra, C. P. Egeland, E. Organista, M. Domínguez-Rodrigo, The origin of the Acheulean: The 1.7 million-year-old site of FLK West, Olduvai Gorge (Tanzania). *Nat. Sci. Rep.* **5**, 17839 (2015).
26. N. Dunbar, G. Zielinski, D. Voisins, Tephra layers in the Siple Dome and Taylor Dome ice cores, Antarctica: Sources and correlations. *J. Geophys. Res.* **108**, 2374–2385 (2003).
27. C. H. Nielsen, H. Sigurdsson, Quantitative methods for electron microprobe analysis of sodium in natural and synthetic glasses. *Am. Mineral.* **66**, 547–552 (1981).
28. J. L. Kirschvink, The least-squares line and plane and the analysis of palaeomagnetic data. *Geophys. J. Roy. Astron. Soc.* **62**, 699–718 (1980).
29. R. A. Fisher, Dispersion on a sphere. *Proc. Royal Soc. London Ser. A* **217**, 295–305 (1953).
30. L. J. Lourens, F. J. Hilgen, J. Laskar, N. J. Shackleton, D. Wilson, in *Geologic Time Scale*, F. M. Gradstein, J. G. Ogg, A. G. Smith, Eds. (Cambridge Univ. Press, 2004), pp. 409–440.
31. V. T. Holliday, *Soils in Archaeological Research* (Oxford Univ. Press, 2004).
32. P. J. Schoeneberger, D. A. Wysocki, E. C. Benham, W. D. Broderson, *Field Book for Describing and Sampling Soils, Version 3.0* (Natural Resources Conservation Service, National Soil Survey Center, 2012).
33. Soil Survey Staff, *Kellogg Soil Survey Laboratory Methods Manual*, R. Burt, Soil Survey Staff, Eds. (Soil Survey Investigations Report No. 42, Version 5.0., U.S. Department of Agriculture, Natural Resources Conservation Service, 2014).
34. S. P. Anderson, W. E. Dietrich, G. H. Brimhall Jr., Weathering profiles, mass-balance analysis, and rates of solute loss: Linkages between weathering and erosion in a small, steep catchment. *Geol. Soc. Am. Bull.* **114**, 1143–1158 (2002).
35. G. H. Brimhall, W. E. Dietrich, Constitutive mass balance relations between chemical composition, volume, density, porosity, and strain in metasomatic hydrochemical systems: Results on weathering and pedogenesis. *Geochim. Cosmochim. Acta* **51**, 567–587 (1987).
36. M. Egli, P. Fitze, Formulation of pedogenic mass balance based on immobile elements: A revision. *Soil Sci.* **165**, 437–443 (2000).
37. G. E. Stinchcomb, L. C. Nordt, S. G. Driese, W. E. Lukens, F. C. Williamson, J. D. Tubbs, A data-driven spline model designed to predict paleoclimate using paleosol geochemistry. *Am. J. Sci.* **316**, 746–777 (2016).
38. W. E. Lukens, L. C. Nordt, G. E. Stinchcomb, S. G. Driese, J. D. Tubbs, B. Barnard, Reconstructing pH of paleosols using geochemical proxies. *J. Geol.* **126**, 427–449 (2018).
39. N. W. Dunbar, R. L. Hervig, Petrogenesis and volatile stratigraphy of the Bishop Tuff: Evidence from melt inclusion analysis. *J. Geophys. Res.* **97**, 15129–15150 (1992).
40. N. W. Dunbar, R. L. Hervig, Volatile and trace element composition of melt inclusions from the Lower Bandelier Tuff: Implications for magma chamber processes and eruptive style. *J. Geophys. Res.* **97**, 15151–15170 (1992).
41. G. Heiken, K. H. Wohletz, *Volcanic Ash* (University of California Press, 1984).
42. P. J. Nilssen, thesis, University of Cape Town (2000).
43. T. E. Cerling, J. G. Wynn, S. A. Andanje, M. I. Bird, D. K. Korir, N. E. Levin, W. Mace, A. N. Macharia, J. Quade, C. H. Remien, Woody cover and hominin environments in the past 6 million years. *Nature* **476**, 51–56 (2011).
44. M. A. Everett, thesis, Indiana University, Bloomington, IN, USA (2010).
45. G. P. Rightmire, M. S. Ponce de León, D. Lordkipanidze, A. Margvelashvili, C. P. Zollikofer, Skull 5 from Dmanisi: Descriptive anatomy, comparative studies, and evolutionary significance. *J. Hum. Evol.* **104**, 50–79 (2017).
46. G. Suwa, Y. Haile-Selassie, T. White, S. Katoh, G. WoldeGabriel, W. K. Hart, H. Nakaya, Y. Beyene, Early Pleistocene *Homo erectus* fossils from Konso, southern Ethiopia. *Anthropol. Sci.* **115**, 133–151 (2007).
47. J. Hawks, M. Elliott, P. Schmid, S. E. Churchill, D. J. de Ruiter, E. M. Roberts, H. H. Wolf, H. M. Garvin, S. A. Williams, L. K. Delezene, E. M. Feuerriegel, P. R. Quinney, T. L. Kivell, M. F. Laird, G. Tawane, J. M. DeSilva, S. E. Bailey, J. K. Brophy, M. R. Meyer, M. M. Skinner, M. W. Tocheri, C. VanSickle, C. S. Walker, T. L. Campbell, B. Kuhn, A. Kruger, S. Tucker, A. Gurtov, N. Hlophe, R. Hunter, H. Morris, B. Peixotto, M. Ramalepa, D. Van Rooyen, M. Tsikoane, P. Boshoff, P. Dirks, L. R. Burger, New fossil remains of *Homo naledi* from the Lesedi Chamber, South Africa. *eLife* **6**, e24232 (2017).
48. E. Bruner, L. Bondoli, A. Coppa, D. W. Frayer, R. L. Holloway, Y. Libsekal, T. Medin, L. Rook, R. Macchiarelli, The endocast of the one-million-year-old human cranium from Buia (UA 31), Danakil Eritrea. *Am. J. Phys. Anthropol.* **160**, 458–468 (2016).
49. E. Abbate, A. Albianelli, A. Azzaroli, M. Benvenuti, B. Tesfamariam, P. Bruni, N. Cipriani, R. J. Clarke, G. Ficcarelli, R. Machiarelli, G. Napoleone, M. Papini, L. Rook, M. Sagiri, T. M. Tecle, D. Torre, I. Villa, A one-million-year-old *Homo* cranium from the Danakil (Afar) Depression of Eritrea. *Nature* **393**, 458–460 (1998).
50. W. H. Gilbert, B. Asfaw, Eds., *Homo erectus*: *Pleistocene Evidence from the Middle Awash, Ethiopia* (University of California Press, 2008).

51. M. G. Leakey, F. Spoor, M. C. Dean, C. S. Feibel, S. C. Antón, C. Kiarie, L. N. Leakey, New fossils from Koobi Fora in northern Kenya confirm taxonomic diversity in early *Homo*. *Nature* **488**, 201–204 (2012).
52. F. Spoor, P. Gunz, S. Neubauer, S. Steler, N. Scott, A. Kwekason, M. C. Dean, Reconstructed *Homo habilis* type OH 7 suggests deep-rooted species diversity in early *Homo*. *Nature* **519**, 83–86 (2015).
53. L. R. Berger, J. Hawks, D. J. de Ruiter, S. E. Churchill, P. Schmid, L. K. Delezene, T. L. Kivell, H. M. Garvin, S. A. Williams, J. M. DeSilva, M. M. Skinner, C. M. Musiba, N. Cameron, T. W. Holiday, W. H. Smith, R. R. Ackermann, M. Bastir, B. Bogin, D. Bolter, J. Brophy, Z. D. Cofran, K. A. Congdon, A. S. Deane, M. Dembo, M. Drapeau, M. C. Elliott, E. M. Feuerriegel, D. G. Martinez, D. J. Green, A. Gurtov, J. D. Irish, A. Kruger, M. F. Laird, D. Marchi, M. R. Meyer, S. Nalla, E. W. Negash, C. M. Orr, D. Radovcic, L. Schroeder, J. E. Scott, Z. Throckmorton, M. W. Tocheri, C. VanSickle, C. S. Walker, P. Wei, B. Zipfel, *Homo naledi*, a new species of the genus *Homo* from the Dinaledi Chamber, South Africa. *eLife* **4**, e09560 (2015).
54. P. H. G. M. Dirks, E. M. Roberts, H. H-Wolf, J. D. Kramers, J. Hawks, A. Dosseto, M. Duval, M. Elliott, M. Evans, R. Grün, J. Hellstorm, A. I. R. Herries, R. J-Boyau, T. V. Makhubela, C. J. Placzek, J. Robbins, C. Spandler, J. Wiersma, J. Woodhead, L. R. Burger, The age of *Homo naledi* and associated sediments in the Rising Star Cave, South Africa. *eLife* **6**, e24231 (2017).
55. M. Dembo, D. Radovčić, H. M. Garvin, M. F. Laird, L. Schroeder, J. E. Scott, J. Brophy, R. R. Ackermann, C. M. Musiba, D. J. de Ruiter, A. Ø. Mooers, M. Collard, The evolutionary relationships and age of *Homo naledi*: An assessment using dated Bayesian phylogenetic methods. *J. Hum. Evol.* **97**, 17–26 (2016).
56. M. F. Laird, L. Schroeder, H. M. Garvin, J. E. Scott, M. Dembo, D. Radovčić, C. M. Musiba, R. R. Ackermann, P. Schmid, J. Hawks, L. R. Berger, D. J. de Ruiter, The skull of *Homo naledi*. *J. Hum. Evol.* **104**, 100–123 (2017).

Acknowledgments: We would like to thank the ARCCH, Ministry of Culture and Tourism, and the Afar State, Ethiopia for the Research permit. L. Morgan and B. Haileab were instrumental in helping with tephra correlations. S.S. would like to thank CENIEH staff, particularly M. J. del Bario and B. de Santiago Salinas for administrative assistance. **Funding:** Major awards and grants were made by G. Getty and the L.S.B. Leakey Foundation. The EU Marie Curie (FP7-PEOPLE-2011-CIG) and MINECO (HAR2013-41351-P) provided major support. Additional funding was provided by the NSF (SBR-9910974 and RHOI BCS-0321893 to T. White and F. C. Howell), the Wenner-Gren Foundation and the National Geographic Society, and major gratitude also to the continuous support of the John and Lois Rogers Trust. In addition, gratitude goes to CRAFT, Stone Age Institute for supporting earlier part of this research. Spanish Government no. CGL2015-65387-C3-1-P (MINECO/FEDER) and Generalitat de Catalunya, AGAUR agency, 2017 SGR 1040 Research Group supported the research by I.C. **Author contributions:** S.S. and M.J.R. organized the project and described the archaeology with D.S. S.W.S. collected, analyzed, and described the hominins. R.L.H. studied the DAN5 endocast. N.E.L., J.Q., R.F.B., N.D., W.C.M., and G.E.S. studied the geology. N.D., N.E.L., and F.H.B. did the tephra correlations. N.E.L., J.Q., and M.E. worked on the stable isotope results, and I.C. and M.E. worked on the taphonomy and fauna, respectively. All authors participated in the writing of the manuscript. **Competing interests:** The authors declare that they have no competing interests. **Data and materials availability:** All data needed to evaluate the conclusions in the paper are present in the paper and/or the Supplementary Materials, and the archaeological and paleontological materials are stored at the National Museum of Ethiopia. Additional data related to this paper may be requested from the authors.

Submitted 21 December 2018
Accepted 19 November 2019
Published 6 March 2020
10.1126/sciadv.aaw4694

Citation: S. Semaw, M. J. Rogers, S. W. Simpson, N. E. Levin, J. Quade, N. Dunbar, W. C. McIntosh, I. Cáceres, G. E. Stinchcomb, R. L. Holloway, F. H. Brown, R. F. Butler, D. Stout, M. Everett, Co-occurrence of Acheulian and Oldowan artifacts with *Homo erectus* cranial fossils from Gona, Afar, Ethiopia. *Sci. Adv.* **6**, eaaw4694 (2020).